Journal of Materials Science: Materials in Electronics (2020) 31:3564–3575
https://doi.org/10.1007/s10854-020-02905-x

Areca catechu extracted natural new sensitizer for dye-sensitized solar cell: performance evaluation

Asmaa Soheil Najm[1] · Norasikin A. Ludin[2] · Mahir Faris Abdullah[3] · Munirah A. Almessiere[4,5] · Naser M. Ahmed[6] · Mahmoud A. M. Al-Alwani[7]

Received: 26 July 2019 / Accepted: 11 January 2020 / Published online: 27 January 2020

Abstract
This paper reports the optical and photovoltaic traits of a new type of natural organic dye sensitizer derived from the Malaysian *Areca catechu* (Pinang) fruit. The photovoltaic potential of this dye was determined by fabricating a dye-sensitized solar cell (DSSC). In this work, the effects of various concentrations of chenodeoxycholic acid (CDCA) and solvent types on the photovoltaic efficiency of this dye were evaluated. Methanol was the best solvent, obtaining the highest absorbance from natural dye. The absorption analyses showed the excellent dye-stabilizing capacity of CDCA. The Fourier-transform infrared spectra revealed the presence of hydroxyl and carboxylic functional groups in the extracted natural dye, which were shown to be responsible for imparting the stronger electronic coupling and rapid electron transfer upon interaction with the TiO_2 surface. The photoluminescence spectral analyses of the dye showed that the inclusion of CDCA as a co-adsorbent can produce a large photocurrent through the narrowing of the band gap. Device performance was measured as a function of co-adsorbent content at the loading times of 0 and 30 min. The efficiency measured after adding CDCA and 30 min of loading time was 0.118%, with short-circuit current density (J_{sc}) = 0.3 mA/cm^2, open circuit voltage (V_{oc}) = 0.536 V, and fill factor (FF) = 73.5%. This short disclosure may contribute towards the development of a natural dye-based efficient DSSC.

1 Introduction

In recent years, the increasingly stringent implementation of environmental laws and the rapid depletion of fossil fuels have compelled mankind to search for environmental amiable materials following the green chemistry route. In this regard, using renewable energy sources is considered a viable solution to gradually reduce the exploitation of fossil fuels, which causes environmental pollution and unsustainable development. Considering these facts, constant efforts have been made to develop efficient photovoltaic technologies, allowing their evolution from first generation (silicon panels) to second generation (thin films), and then to third-generation dye-sensitized solar cells (DSSCs). These DSSCs provided the basis for developing fourth-generation solar cells (SCs) [1] and different components of the DSSC technology.

Intensive research has been conducted to raise the overall efficiency and durability and decrease the cost of DSSCs by improving their major components including anodes, counter electrodes, electrolytes, and photosensitizers [2]. The photosensitizer is an important part of a DSSC, and has the function of absorbing sunlight and converting it

✉ Naser M. Ahmed
naser@usm.my

1 Department of Electrical Electronic & Systems Engineering, Faculty of Engineering and Built Environment, Universiti Kebangsaan Malaysia, UKM Bangi, 43600 Bangi, Selangor, Malaysia

2 Solar Energy Research Institute (SERI), Universiti Kebangsaan Malaysia, UKM Bangi, 43600 Bangi, Selangor, Malaysia

3 Department of Refrigeration and Air Conditioning, AL-Rafidain University College, Baghdad, Iraq

4 Department of Physics, College of Science, Imam Abdulrahman Bin Faisal University, P.O. Box 1982, Dammam 31441, Saudi Arabia

5 Department of Biophysics, Institute for Research and Medical Consultations (IRMC), Imam Abdulrahman Bin Faisal University, P.O. Box 1982, Dammam 31441, Saudi Arabia

6 School of Physics, Universiti Sains Malaysia, USM Penang, 11800 Penang, Malaysia

7 Department of Biology, College of Education for Pure Sciences/Ibn Al-Haitham, University of Baghdad, Baghdad, Iraq

into electrical energy [3]. Therefore, many novel sensitizers including ruthenium dyes, porphyrin dyes, and metal-free organic dyes have been developed and performed well. Significantly, record high efficiencies of 12.75% and 13.00% [4] have been achieved with zinc porphyrin dye, which are higher than the remarkable conversion efficiency at 11% of ruthenium sensitizers, such as N_3, N719, and black dye [5]. However, the expensive and scarce nature of artificial dyes limits their widespread application in DSSCs. Moreover, using these dye compounds, obtained from the natural environment, leads to substantial environmental load [6, 7]. Thus, it is conceivable to utilize naturally available dyes as alternative photosensitizers in a DSSC and achieve significant efficiencies. The advantages of natural dyes over synthetic ones are their accessibility, abundance, and availability; they do not require refinement and purification, are non-pollutants, and impressively decrease the cost of devices [8].

The plant-extracted natural dyes are observed to be more prospective owing to their abundance and eco-friendly characteristics. Substations of natural dyes as sensitizers were shown to be not only economically viable and nontoxic but also effective for enhancing efficiency up to 11.9% [9]. Sensitizers for DSSCs need to fulfill important requirements such as absorption in the visible and near-infrared regions of the solar spectrum and strong chelation to the semiconductor oxide surface. Moreover, the lowest unoccupied molecular orbital (LUMO) of the dye should lie at a higher energy level than the conduction band of the semiconductor so that, upon excitation, the dye could introduce electrons into the conduction band of the TiO_2 [10]. Considering the above, we targeted an abundant and cheap Malaysian fruit, betel nut (*Areca catechu*), to obtain a new natural dye to use as a sensitizer in DSSCs. This fruit contains tannins, polyphenols, gallic acid, catechins, alkaloids, fat, gum, and other minerals. Gallotannic acid, a stable dye, is the main pigment (yellowish) of *A. catechu* and is responsible for the effective absorption of visible wavelengths; thus, it is useful as a sensitizer in DSSCs [11]. The visible photons absorbed by the dye molecules create charge carriers (electric current) and transfer electrons to the TiO_2 material [12].

Various types of additives have currently been mixed with dye solutions to improve the photovoltaic performance (both the photocurrent and photovoltage) of the fabricated DSSCs. These additives (acting as co-adsorbents) include cholic acid with porphyrin derivatives, 3-phenylpropionic acid (PPA), hexadecylmalonic acid (HDMA), deoxychoic acid (DCA), 1-decyl phosphoric acid (DPA), and chenodeoxycholic acid (CDCA) [13–15]. Amongst all these co-adsorbents, CDCA is the most versatile and popular one. CDCA is a natural saturated polycyclic molecule enclosing a four-carbon chain that separates a sterol nucleus from the carboxylic acid-anchoring group [16]. CDCA has two significant characteristics: its cost-effectiveness and strong attachment capacity to mesoporous TiO_2 nanostructures, which are responsible for hindering dye accumulation and transfer of dye molecules on the semiconductor surface [13]. Using CDCA, it is possible to inhibit dye collection and enhance electron transfer. This in turn improves the performance of the DSSC and enhances its efficiency. Additionally, the presence of CDCA improves the photovoltage owing to the reduction of the charge recombination [17].

Jungsuttiwong et al. investigated the effects of CDCA as a co-adsorbent in a dye solution on the photovoltaic performance of DSSCs. It was found that the co-adsorption of CDCA hinders the formation of dye aggregates, improves electron injection yield and J_{sc}, and dramatically increases efficiency up to 6.51% [18].

Based on these factors, the present work evaluated the optical and photovoltaic properties of a new type of natural organic dye sensitizer extracted from the *A. catechu* fruit by incorporating it into a fabricated DSSC for the first time. The detailed characterization of the optical and photovoltaic properties of this natural dye revealed its effectiveness for application in DSSCs. This natural green sensitizer derived from the cheap and abundant Malaysian fruit *A. catechu* (Pinang) was shown to have the potential to realize efficient performance of DSSCs. The photovoltaic performance of the *A. catechu*-derived dye incorporated into a DSSC was optimized as a function of CDCA concentration (used as co-adsorbent). The photovoltaic potential of this dye was interpreted using the mechanisms of the CDCA adsorption onto the substrate surface, absorption spectral evolution, energy level alignment, and charge transfer.

2 Experiment

2.1 Pinang fruit as source of dye sensitizer

Figure 1 shows the Malaysian Pinang fruit used to extract the new natural dye. The Pinang plant is classified as follows: Kingdom: Plantae; Order: Arecales; Family: Arecaceae; Genus: *Areca;* Species: *Catechu.* Generally, this palm species of *A. catechu* (locally called the betel tree) is found in the tropical regions of Asia and eastern Africa [19]. The seed of this fruit, which is enriched in alkaloids (including arecaidine and arecoline), is often sliced and chewed (endosperm) as a mild stimulant. It has antidepressant properties in rodents [20, 21].

Areca catechu contains different types of sugars, lipids, and polyphenols [22]. In *A. catechu,* the most bio-active elements are the polyphenols, which include tannins, hydrolysable tannins, and flavonols. Figure 2 displays the structure of the chemical compound called catechin found in *A. catechu*.

Fig. 1 Malaysian Pinang fruit

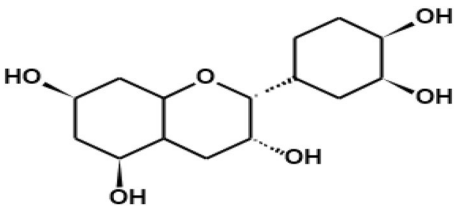

Fig. 2 Chemical structure of catechin in *A. catechu*

2.2 Preparation of sensitizers from *A. catechu*

Following the earlier protocol described in [23], we prepared the natural dye. Fresh fruit was obtained from Pinang, Malaysia. The Pinang fruit used in this research belongs to a big orange species. The fresh fruits were washed repeatedly with water to remove dust, and their crusts were removed. The crusts were allowed to dry first at 25 °C in shade, and then in an oven at 40 °C for 24 h, until the crusts became crisp. After drying, the crusts were crushed in a grinder (Mulry function disintegrator SY-04) to obtain a powder. A total of 40 g of the powder was added to 400 mL of five different solvents (methanol, ethanol, chloroform, acetonitrile, and hexane), and then the extracted solution was placed in a shaker (Ambient Shaker Incubators, SKU: SI-100) for 24 h. The extract solution was filtered using filter paper (NICE, 12.5 cm, 102 Qualitative). Finally, the derived dye solution, without further isolation or purification, was used as natural sensitizer for the fabricated DSSCs.

2.3 Chenodeoxycholic acid (CDCA) synthesis

The natural *A. catechu* dye extract (200 mL) in methanol was divided into four conical flasks. Then, the CDCA powder (Solaronix) was added to each flask at different concentrations (0.1, 0.5, 1.0, and 1.5 mM) and equilibrated for 15 min. Finally, these samples were analyzed.

2.4 Preparation of dye-sensitized solar cell

The TiO_2 porous film electrode was prepared using a modified method based on those published in [24, 25]. A TiO_2 paste was prepared by blending 3.0 g of commercial TiO_2 anatase (supplied by ALDRICH), 6.0 mL of nitric acid (0.1 M), and 1.0 g of polyethylene glycol (MW 10,000) using a mortar and pestle. Each paste was ground for about 30 min, and then several drops of a nonionic surfactant, Triton X-100 (supplied by SIGMA) were added while continuously stirring the mixture. After cleaning the conductive glass using ethanol, an adhesive tape was used to fix it onto a flat surface. Moreover, the tape controlled the thickness and the area of the TiO_2 film. Several drops of the resultant TiO_2 pastes were spread onto an area of about 1 cm^2 of the conductive glass using a glass rod through the doctor blade procedure [26]. After drying, the TiO_2-coated conductive slide was solidified and sintered at 450 °C for 30 min in a furnace (LENTON THERMAL DESIGHN, England). Heat treatment increased the compactness of the thin film while sintering of the photoelectrode at 450 °C created the electronic contact between the TiO_2 particles. After the TiO_2 cooled to about 80 °C, the thin films were immersed into each dye solution for 24 h at room temperature under a dark condition. The electrode was washed with ethanol to remove other impurities and the porous TiO_2 was dried in moisture-free air to remove excess water.

2.5 Assembling of DSSC

A DSSC mainly consists of an anode electrode (conductive glass, TiO_2 porous film, natural dye), an electrolyte, and a cathode electrode (conductive glass, Pt-catalyst). DSSCs were assembled by placing the dry TiO_2-coated slide on a flat surface such that TiO_2 faced up and the counter electrode slide faced down on top of the electrode. After holding the two electrodes in this orientation using two binder clips, a liquid electrolyte (0.5 M potassium iodide mixed with 0.05 M iodine dissolved in a solution of ethylene glycol + acetonitrile with a volume ratio 4:1) was drawn between the dried film electrode (anode electrode) and the counter electrode (cathode electrode) by capillary action. The excess electrolyte solution was wiped from the exposed areas of the glass cell because it could affect the performance of the cell.

2.6 Characterization and measurements

There are several methods to characterize the sensitizer with CDCA. One important characteristic of a sensitizer is its absorption strength and wavelength range, which was determined by subjecting the extracted solution of *A. catechu* dye to a UV–Vis spectrometer (Perkin Elmer, Lambda 35).

Another method of characterization is Fourier-transform infrared (FTIR) spectroscopy (Model NICOLET 6700 FTIR) in the wavenumber region of 4000–400 cm^{-1} to assign the observed spectral characteristics of functional groups corresponding to different absorption bands that are responsible for the absorption. The photoluminescence (PL) emission spectra of the dye suspension were measured using a fluorescence spectrometer 50560. This technique is widely used to investigate the energy levels of materials by providing fundamental information on the electronic properties and impurity levels of these materials. One of the most accurate methods to characterize organic materials and estimate the energy band diagram is cyclic voltammetry (CV), which was conducted using a Solartron system (Model: Modulab H032850). In this test, three electrodes such as the working (Pt-formed FTO substrate or glassy carbon), counter (Pt), and reference (Ag+/AgCl) were utilized, wherein a phosphate buffer solution (PBS of 0.2 M at pH 7.2) served as the electrolyte. The voltage was varied in the range of − 1.0 to + 1.0 V at a scan rate of 50 mVs^{-1} to record the data. The incident photo–current conversion efficiency (IPCE) of the DSSCs in the range of 300–1100 nm was measured using a calibrated photodiode (Pembuat: UK, Jenama: Bentham, Model: PVE300 EQE (ICPE) IQE). IPCE is a measure of how well the device converts light to current at a specific wavelength. The current voltage (I–V) characteristics of the DSSCs were obtained (I–V Tester: XES – 40S1 S/N: 074, Keithley 2400 Source Meter Model 2401) under the direct solar illumination at an irradiance of 100 Wm^{-2}. Based on the photo-current–voltage (I–V) curve, fill factor (FF) can be estimated using the formula:

$$FF = \frac{I_{max} * V_{max}}{J_{sc} * V_{oc}} \quad (1)$$

Here I_{max} and V_{max} are the photocurrent and photovoltage for P_{max} (maximum power output), J_{sc} is the short-circuit photocurrent, and V_{oc} is the open circuit photovoltage. The overall solar conversion efficiency (η) of a DSSC is defined as

$$\eta = \frac{J_{sc} * V_{oc} * FF}{P_{in}} \quad (2)$$

where P_{in} is the input power.

3 Results and discussion

3.1 Effects of solvents and CDCA on the absorbance of extracted dye

Figure 3 shows the types of solvent (hexane, acetonitrile, ethanol, methanol, and chloroform) dependent UV–Vis spectra of the natural *A. catechu* dye sensitizer, which consisted of three broad peaks at 422, 445, and 470 nm. The observed strong absorption by the natural dye in different solvents after being stored at room temperature over a period of 72 h under a dark condition indicated its effectiveness as a sensitizing agent. This strong absorption in the UV–Vis

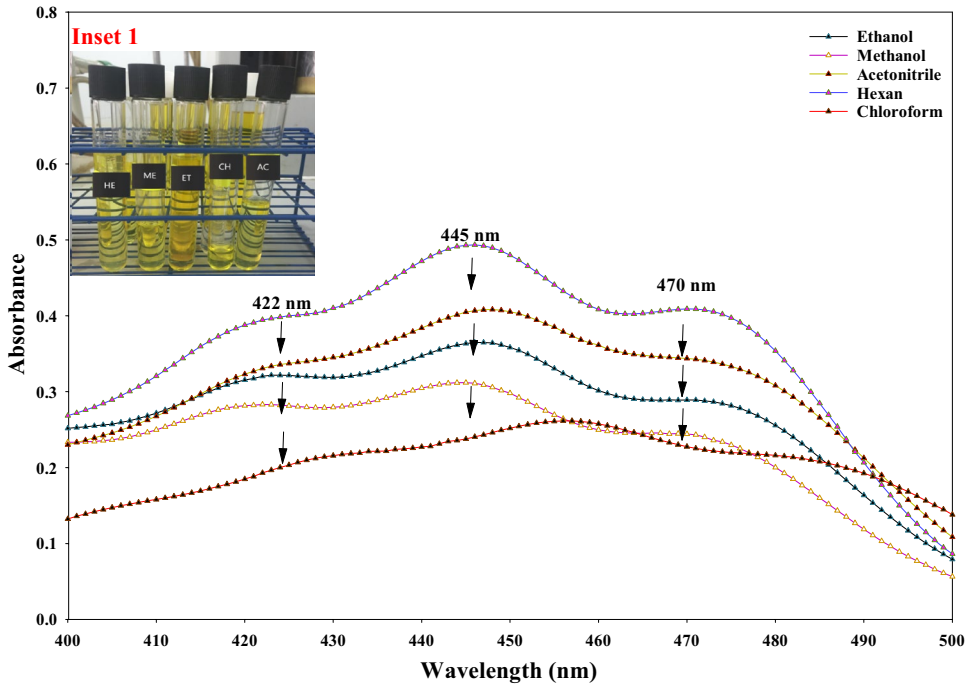

Fig. 3 Effects of different solvents on the UV–Vis absorption spectra of *A. catechu* dye suspension

region by the dye molecules with high content was attributed to their chemical structures and the solvent polarities of methanol and ethanol. Despite the non-polar nature of hexane, it produced the maximum absorption as indicated in the preparative chromatography [27]. These results were in agreement with that of Petricevich et al., who reported that hexane with Zero Polarity Index can extract only lipophilic compounds from solute molecules [28]. Indeed, the concentration of the extracted dye in the solutions is strongly dependent on the nature of the solvent because of the variety of chemical compounds present in plant materials, and solvent polarities determine whether certain compounds are soluble in a particular solvent. Based on the above, we selected methanol as the organic polar solvent to extract the *A. catechu*-based natural dye sensitizer.

Figure 4 illustrates the CDCA content-dependent UV–Vis spectra of the *A. catechu* dye suspension in a methanol solvent. It is comprised of three distinct peaks at 422, 443, and 467 nm accompanied by broadening. The most intense peak at 443 nm revealed a hyperchromic shift. The dye suspension containing 0.1 mM of CDCA exhibited the highest absorbance, indicating the improvement in the absorption intensity due to the inclusion of CDCA as co-adsorbents. It was confirmed that CDCA is an excellent stabilizing agent for the natural dye [29]. However, when the concentration was increased, the absorbance was quenched. Our results are in agreement with those of Hassan et al. [30], showing that the quenching of the absorption intensity of the dye at a higher concentration of CDCA was due to the competition between the two compounds that occurred on the TiO_2 surface. In fact, the strong interactions amid the adsorbed dyes and the TiO_2 molecules caused the aggregations of dyes, thereby contributing to the observed broadening (widening of the full width and half maximum) in the absorption spectral profile. In addition, Yum et al. found that the use of co-adsorbents for the coating of dyes is an excellent strategy to overcome the issues related to the aggregations of dyes, which is responsible for the inhibition of the generation of photocurrent [16].

Generally, our dye exhibits an absorption band in the range of visible light because of the charge-transfer transition from the highest occupied molecular orbital (HOMO) in the ground state to the LUMO in the excited state; hence, we can consider it as a suitable material for a photosensitizer in the visible light region.

3.2 FTIR spectral analyses

Figure 5 displays the CDCA concentration-dependent FTIR spectra (in the range of 900–3600 cm^{-1}) of the *A. catechu* dye suspension in methanol media. The presence of functional chemical groups and their bonding vibrations in the spectral profile provided the detail signature involving the interaction between CDCA and the natural dye molecules. The appearance of the vibration band at 1021.25 cm^{-1} was due to the ether (C–O–C) and carboxylic acid stretching. The observed vibration band at 1422.87 cm^{-1} was due to the bending of O–H and aldehyde. The bands occurring at 2832.01 cm^{-1} and 3314.03 cm^{-1} were due to the stretching of C–H and amine, respectively [31]. These results are consistent with the earlier report related to the observation of six hydroxyl groups in delphinine, wherein it was argued that the presence of anthocyanidin molecules is useful for strong binding with TiO_2 surface [32].

All the samples revealed similar transmittance profiles in terms of various functional group co-ordinations irrespective of the varying CDCA contents. Additionally, CDCA exhibited a tendency to form strong intermolecular hydrogen

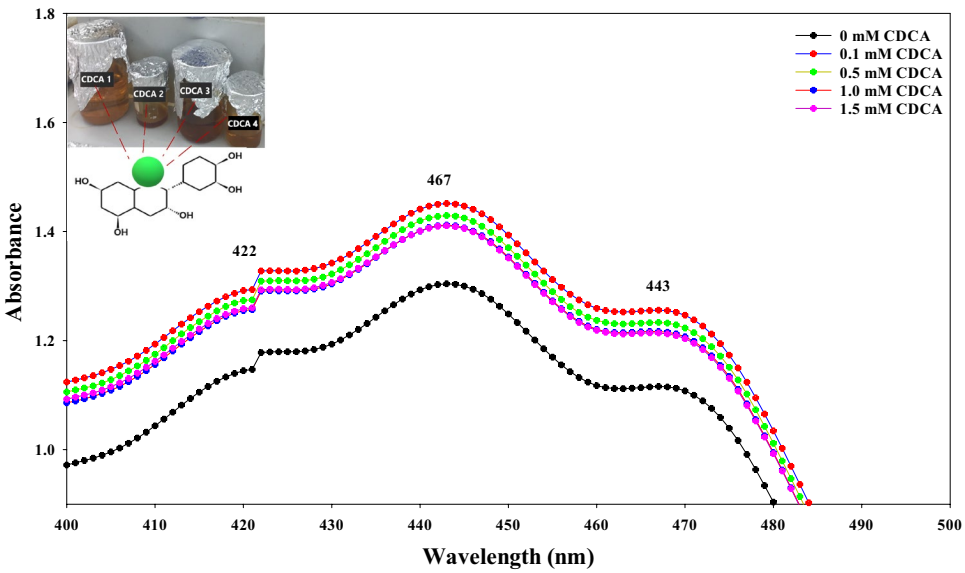

Fig. 4 CDCA concentration-dependent UV–Vis spectra of *A. catechu* dye suspension in methanol

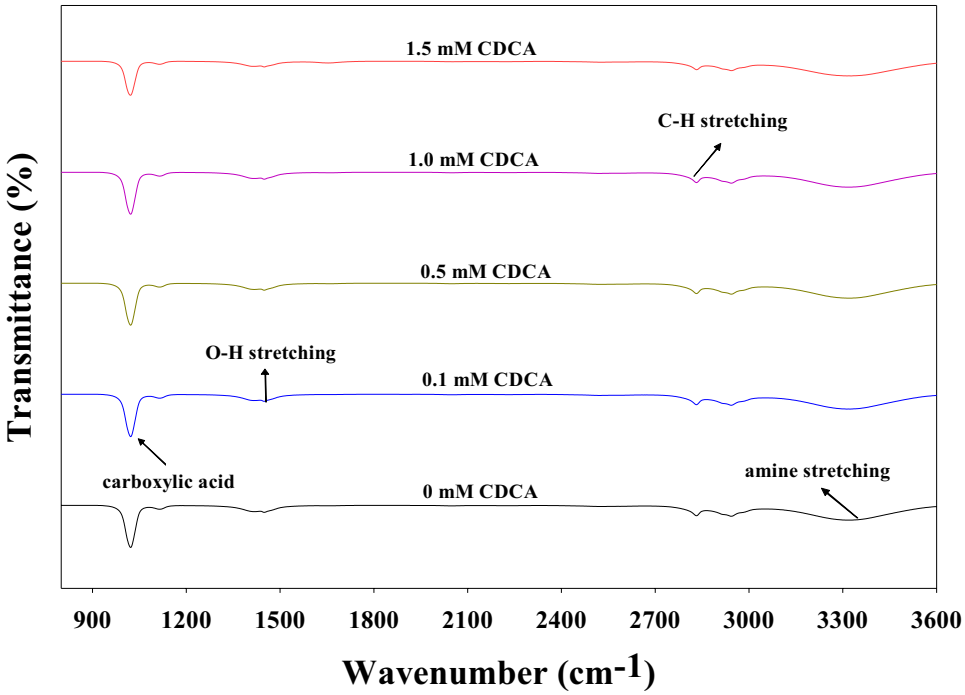

Fig. 5 FTIR spectra of CDCA included *A. catechu* dye suspension in methanol

bonds, which led to the formation of extensive crystal network arrangements [33]. The presence of the carboxylic acid stretching vibration and carboxylic groups with hydrogen bonds in all samples confirmed the existence of the intermolecular aggregations. These results are consistent with the results reported by Ismail et al. [34], who found that the inclusion of CDCA to various contents of mangosteen fruit extract showed an improvement in the device function. This observation was ascribed to the CDCA inclusion-assisted formation of extra –OH bonds in the dye sensitizer that could attach onto the conductive surface of titania. Briefly, the occurrences of different transmittance bands authenticated the successful adsorption of CDCA onto the TiO_2 surface and the modification of the chemical structures useful for efficiency enhancement of the cell. The enclosures of the C=O, –OH, and –COOH groups in all the prepared dye suspensions served as effective charge carriers in the fabricated DSSC and responsible for the enhanced photovoltaic performance when illuminated.

3.3 Photoluminescence spectra of *A. catechu* dye

Figure 6 depicts the PL emission spectra of the *A. catechu* dye suspension in methanol as a function of different CDCA concentrations. All the samples showed a broad emission peak, indicating the probability of weak electron–hole recombination process. The spectral peak occurring between 650 and 700 nm showed a blue-shift. The PL peak (at approximately 667 nm) for the dye suspension without containing CDCA occurred at a much lower wavelength compared to those incorporated with CDCA. This peak wavelength (λ) was used to estimate the energy band gap (Eg) of the dye through the relation:

$$E_g = \frac{hc}{\lambda} \tag{3}$$

where h is Planck's constant ($6.62607004 \times 10^{-34}$ m^2 kg s^{-1}) and c is the speed of light (3.0×10^8 m s^{-1}).

The PL intensity of the *A. catechu* dye suspension without any additive was lower than those with CDCA, suggesting the lower recombination rate of the photogenerated carriers of the pure dye. This observation was ascribed to the entrapment of holes by the oxygen vacancies, wherein such trapping may result in the lower nobilities of holes than normal cases, improving the mobility of the electrons and thereby decreasing the recombination of carriers. These results were in agreement with the previous investigation of Mercado et al. [35]. However, the observed red shift in the PL peak intensity for the dye containing CDCA was mainly ascribed to the creation of the Schottky barrier at the CDCA–dye interface. This barrier in turn acted as a sink for electrons and hindered the recombination of electrons and holes [36], promoting the enhanced photovoltaic performance. In summary, the examination of the photoluminescence showed broadening intensity at various concentrations of CDCA due to the alterations in the structures of the chemical compounds of the *A. catechu* dye suspension in methanol.

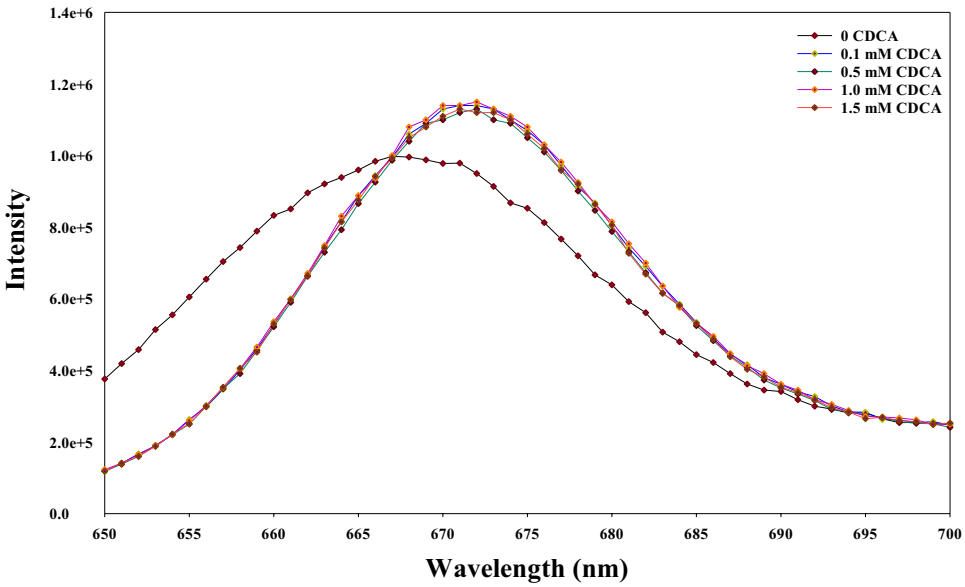

Fig. 6 PL spectra of CDCA included *A. catechu* dye suspension in methanol

3.4 Electrochemical traits of CDCA-blended *A. catechu* dye

The effects of various CDCA contents on the electrochemical traits of the *A. catechu* dye sensitizer suspension were examined using CV analyses, Fig. 7. This test provided detailed information related to the redox behaviors of the *A. catechu* dye in terms of the electron transport mechanisms from the excited dye molecules to the conduction band (CB) of TiO_2 [37]. The onset of the oxidation acquired from the extrapolation of the CV graph and the value of band gap obtained from the PL spectral analyses were further used to estimate the HOMO and LUMO levels (in eV) of the *A. catechu* dye following the relations [38]:

$$E_{\mathrm{HOMO}} = -e\left(E_{\mathrm{ox}}^{\mathrm{onset}} + 4.4\right) \tag{4}$$

$$E_{\mathrm{LUMO}} = E_{\mathrm{HOMO}} + E_{\mathrm{g}} \tag{5}$$

The estimated result, as displayed in Table 1, shows that CDCA affects the HOMO and LUMO levels. The range of LUMO is between − 2.7 and − 2.81 eV and that of HOMO is between − 4.56 and − 4.66 eV. On average, the E_g between each HOMO and LUMO is 1.85 eV, which is the amount of energy for photo responsive when the photon is absorbed into the sensitizer.

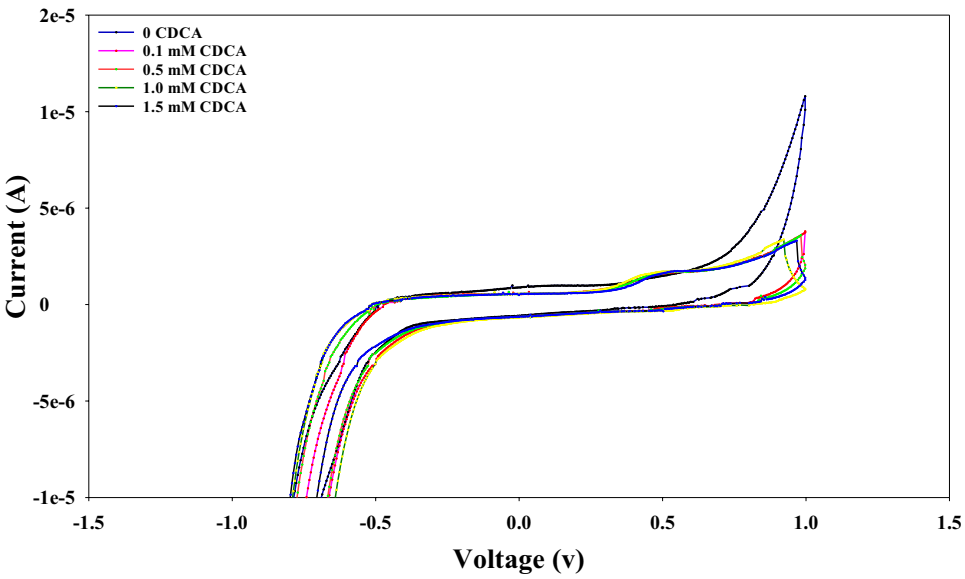

Fig. 7 Cyclic voltammetry curve for characteristics of the CDCA-incorporated *A. catechu* dye suspension in methanol

Table 1 CDCA content-dependent absorption and CV properties of the *A. catechu* dye suspension

Criterion	Pure dye	Dye + 0.1 mM CDCA	Dye + 0.5 mM CDCA	Dye + 1.0 mM CDCA	Dye + 1.5 mM CDCA
Wavelength (nm)	444	444	444	445	444
Absorbent (a.u.)	1.303	1.450	1.428	1.406	1.409
Carboxyle group	(2943.56, 2832.03, 1115.03, 1021.98)	(2943.90, 2832.61, 1653.80, 1114.88, 1021.36)	(2943.72, 2832.02, 1114.75, 1021.96)	(2943.82, 2832.12, 1114.92, 1021.92)	(2943.48, 2831.85, 1114.99, 1022.09)
Bandgap (eV)	1.864	1.845	1.848	1.850	1.853
HOMO (eV)	4.563	4.603	4.623	4.637	4.667
LUMO (eV)	2.699	2.758	2.775	2.787	2.814

The results indicated that the LUMO of the dye was effective in imparting sufficient thermodynamic potential for the injection of electrons from the excited molecular states to the CB of TiO_2. The CV analyses revealed that the HOMO energies of all the CDCA-incorporated dyes were lower than the I^-/I^{-3} potential, suggesting the adequacy of the driving force for their carrier's regeneration [39]. The narrower the energy band gap, the higher was the absorption and extinction coefficient of the dye. In fact, the band gap of the dye was considerably reduced owing to the incorporation of CDCA. The present finding is consistent with a previous report [40]. This finding is in agreement with that of Su'ait et al., who found that CDCA caused a shift in the anodic and cathodic peaks owing to the intermolecular interactions mediating the filling of the surface states of CDCA, indicating higher oxidation potentials (existence of deeper HOMO energy level) [41]. The present observation also suggested that the intercalation of CDCA particles into the dyes improves charge transfer owing to the higher conductivity of the dye and the interfacial energy level equilibration [42]. The CV curves of all samples showed a redox reaction with broad and symmetrical redox waves, wherein the electro-growth obtained with the varying concentrations may increase the redox behavior. In particular, the dye containing 1.5 mM of CDCA showed optimum HOMO and LUMO levels and visible absorption intensity compared to the other dyes (Table 1). Hence, it was selected as the best concentration for DSSC fabrication.

3.5 Incident photon to current efficiency (IPCE) of the DSSC

Figure 8 compares the IPCE performance of the SC sensitized with the pure *A. catechu* dye with the one incorporated with the optimum concentration of CDCA at 1.5 mM. For both cases, the onset of IPCE was at approximately 340 nm. The value of IPCE of the proposed DSSC was evaluated using [43]

$$\mathrm{IPCE}(\%) = \frac{1240(\mathrm{eV\,nm}) \times J}{\mathrm{I} \times \lambda} \times 100\% \tag{6}$$

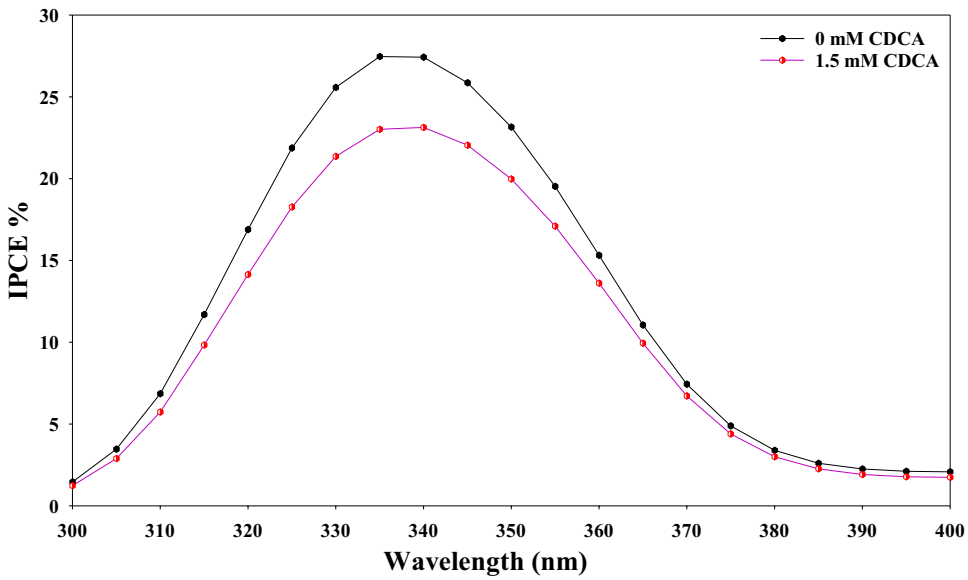

Fig. 8 IPCE curves for the DSSC sensitized with pure dye and the optimum one containing 1.5 mM of CDCA

where I (mW cm^{-2}) is the incident monochromatic light irradiance, J (mA cm^{-2}) is the short-circuit current density, and λ (nm) is the wavelength of the incident monochromatic light.

It was inferred that the optimization of the dye sensitizer through the co-adsorbent CDCA is an effective strategy to inhibit dye aggregation, lowering the rates of charge recombination, thereby enhancing IPCE values. The maximum IPCE of the cell incorporated with pure *A. catechu* dye was 27.46%; however, after 5 days of soaking in the pure dye with CDCA, the IPCE was reduced to 25.78%. The observed marginal drop in the IPCE value after the inclusion of CDCA was ascribed to the overloading of the sensitizer mediated by aggregation on the TiO_2 film. This limitation is considered as the major reason for the lowering of IPCE. Such a mechanism may produce a strong imbalance between the rates of electron transport in the TiO_2 and the recombination of photo-injected electrons with I^{3-} in the electrolyte [44]. The disparity in IPCE values for different natural dyes can be ascribed to the varying quantities of natural dye loading onto the TiO2 surface. agreement with previous studies which found that this is in degrees of charge carrier recombination and excited energy states vary depending on the properties of natural dyes molecules [45].

3.6 Current–voltage characteristics of the DSSC

Figure 9 displays the I–V curves of the SC sensitized with pure dye and the one containing the optimum content of CDCA (1.5 mM) recorded at two different times. The I–V measurement was performed under the solar illuminations of AM 1.5 to evaluate the photovoltaic parameters. The performance of the SC sensitized with the *A. catechu* natural dye was evaluated in terms of open circuit voltage (*Voc*), short-circuit current density (J_{sc}), maximum power (P_{max}), FF, and overall efficiency (η) as indicated in Table 2.

The value of η for the dye included cell activated without and with 1.5 mM of CDCA was approximately 0.077% and 0.068%, respectively. This lower value of η for the cell due to co-adsorbent activation in the dye is attributed to the insufficient number of attaching groups for carrier transport, which reduced the photovoltaic performance. Consequently, the value of J_{sc} also dropped owing to the deficiency of anchoring groups required for the transfer of charge carriers, thereby reducing electron diffusion from the dye molecules to the TiO_2 surface. The addition of more CDCA may increase the number of electrons by increasing the number of conductive channels and attaching groups among the dye sensitizer molecules and the conducting surface of TiO_2 [46]. Moreover, at very high CDCA contents, the value of V_{oc} does not change significantly, suggesting that CDCA does not improve the recombination activity performance [47].

This result is in agreement with those reported by Pugliese et al. who found an increase in J_{sc} after the addition of a co-adsorbent during the loading times due to the improved electron injection efficiency into the cell [48]. Thus, the

Table 2 Photo-electrochemical parameters of the SCs (under white light illumination at intensity of 1000 W/m^2) sensitized with pure dye and the optimum one containing 1.5 mM of CDCA

DSSC	CDCA (mM)	J_{sc} (mA/cm^2)	V_{oc} (V)	FF (%)	η (%)
At time 0	0	0.2	0.539	72.53	0.077
	1.5	0.2	0.530	64.73	0.068
After 30 m	0	0.3	0.540	76.37	0.123
	1.5	0.3	0.536	73.51	0.118

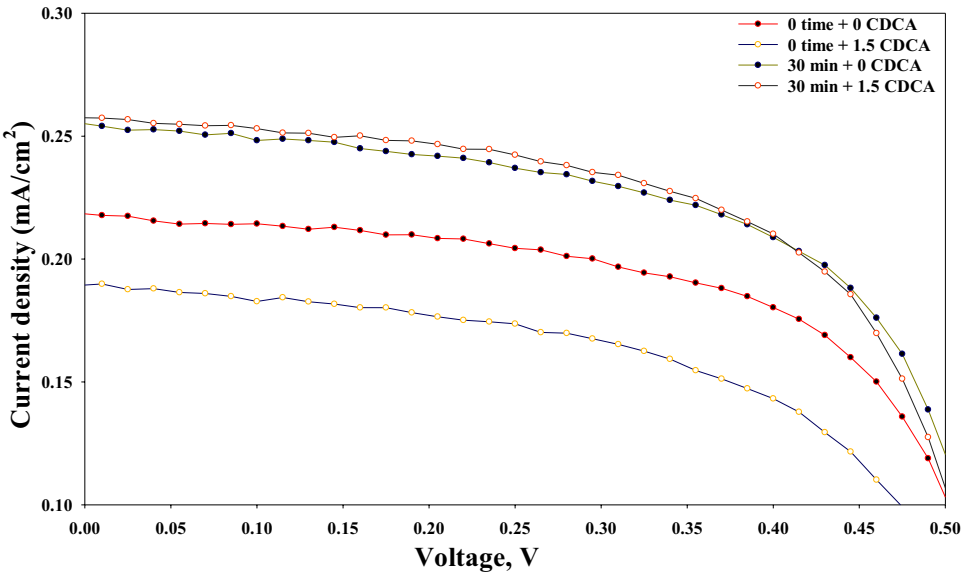

Fig. 9 I–V curves of the DSSC sensitized with pure dye and the optimum one containing 1.5 mM of CDCA

Table 3 Photo-electrochemical parameters of the natural dye-based DSSC extracted from different plants

Natural dye	J_{sc} (mA cm^{-2})	V_{oc} (V)	FF	η (%)	References
Eggplant peels	3.4	0.35	40	0.47	[50]
Tangerine peels	0.74	0.59	63	0.27	[51]
Annatto	0.53	0.56	66	0.19	[52]
Rosella	1.63	0.40	57	0.37	[53]
Dragon fruit	0.20	0.22	30	0.22	[54]
Ipomoea	0.91	0.54	0.56	0.28	[55]
Delonix regia	1.33	0.30	0.39	0.317	[56]
Begonia	0.63	0.537	0.72	0.24	[51]
Spinach	1.12	0.565	0.59	0.318	[57]
Cherries	0.466	0.565	0.38	0.181	[58]
K. japonica	0.5597	0.5839	0.68	0.22	[59]

duration of 30 min was chosen for dye loading. This time was enough to attain a lower resistance for the SC sensitized with the CDCA-incorporated dye, confirming its benefit against the suppression of dye aggregation responsible for the reduced electron injection [49]. Moreover, with the elongation of loading time, the disaggregation process was completed, where CDCA was responsible for the conflicting mechanism. This conflict in turn prevented the effective attachment of the dye sensitizer onto the semiconductor surface, thereby improving cell efficiency. In spite of the substantial improvement, the inadequacy of time could not increase the efficiency difference further from 0.123 to 0.118% for the cell without and with CDCA inclusion, respectively, which should be considered as another factor to be improved to obtain a higher efficiency from *A. catechu*. Table 3 compares the evaluated values of the photochemical parameters of the metal complexes (natural dyes) extracted from various plants and incorporated into DSSCs.

4 Conclusions

The photo-electrochemical characteristics of a new type of natural organic dye sensitizer extracted from the Malaysian *A. catechu* (Pinang) fruit was reported for the first time. The photovoltaic efficiency of this dye was evaluated by fabricating a DSSC. The influence of varying contents of CDCA and solvent types on the photovoltaic efficiency of this dye was quantified. The dye adsorption and sensitization was optimized through the introduction of the CDCA co-absorbent at various concentrations. The optimal performance of the cell was achieved at 1.5 mM of CDCA. The inclusion of CDCA was effective in increasing the attachments of charge transporting groups within the dye molecules, thereby enhancing the electron transfer among the photosensitizer molecules and the TiO_2 surface. The *A. catechu* sensitizer was subjected to UV–Vis spectrometry to determine the absorption spectra for each sensitizer in different solvents. Methanol was chosen owing to its polarity. The CV curve was used to indicate the HOMO and LUMO for each sensitizer. The photochemical properties were supported by the IPCE measurement whereas the highest IPCE was obtained at 27.46% using the pure *A. catechu* sensitizer and 25.78% with CDCA. Results showed that after adding CDCA, the properties dropped. This observation was ascribed to the dye aggregations onto the TiO_2 surface, affecting the effective charge-transfer process. In future studies, the loading time for CDCA should be optimized to reduce aggregation. The photovoltaic performance was measured as a function of co-adsorbent content at the loading time of 30 min. A maximum photo conversion efficiency of 0.123% at 30-min loading time without the co-adsorbent was achieved, which decreased to 0.118% upon the addition of 1.5 mM CDCA. In conclusion, CDCA is capable of being used as a catalyst to increase the performance of a DSSC by creating more pathways for photocurrent conversion and to increase the range of photocurrent conversion spectra by providing more anchoring capabilities for the natural dye. However, these should take effect once loading time has been optimized. For the reference of other researchers, the modification of the dye structure using CDCA could produce enhanced visible light absorption, indicating its benefits for DSSCs.

Acknowledgements The authors are thankful to the School of Physics at USM University for supporting this research trough the Bridging grant (304.PFIZIK.6316276).

Compliance with ethical standards

Conflict of interest The authors declare that there is no conflict of interest regarding the publication of this paper.

References

1. K. Nazeeruddin, E. Baranoff, M. Gra, Dye-sensitized solar cells: a brief overview. Sol. Energy **85**, 1172–1178 (2011)
2. Y. Bai, Y. Cao, J. Zhang, M. Wang, R. Li, P. Wang, S.M. Zakeeruddin, M. Grätzel, High-performance dye-sensitized solar cells based on solvent-free electrolytes produced from eutectic melts. Nat. Mater. **7**(8), 626 (2008)
3. Y. Chiba, A. Islam, Y. Watanabe, R. Komiya, N. Koide, L. Han, Dye-sensitized solar cells with conversion efficiency of 11.1%. Jpn. J. Appl. Phys. **45**(24–28), 23–26 (2006)
4. S. Mathew, Y. Aswani, P. Gao, R. Humphry-Baker, B.F.E. Curchod, N. Ashari-Astani, I. Tavernelli, U. Rothlisberger, M.K. Nazeeruddin, M. Grätzel, Dye-sensitized solar cells with 13% efficiency achieved through the molecular engineering of porphyrin sensitizers. Nat. Chem. **6**(3), 242 (2014)
5. M. Grätzel, Conversion of sunlight to electric power by nanocrystalline dye-sensitized solar cells. J. Photochem. Photobiol. A **164**(1–3), 3–14 (2004)

6. A. Gürses, M. Açıkyıldız, K. Güneş, M.S. Gürses, *Dyes and Pigments: Their Structure and Properties* (Springer, Cham, 2016)
7. S. Sharma, B. Siwach, S.K. Ghoshal, D. Mohan, Dye sensitized solar cells: from genesis to recent drifts. Renew. Sustain. Energy Rev. **70**, 529–537 (2017)
8. M.Z. Iqbal, S.R. Ali, S. Khan, Progress in dye sensitized solar cell by incorporating natural photosensitizers. Sol. Energy **181**, 490–509 (2019)
9. M.A. Green, H. Yoshihiro, E.D. Dunlop, D.H. Levi, J. Hohl-Ebinger, M. Yoshita, A.W.Y. Ho-Baillie, Solar cell efficiency tables (version 53). Prog. Photovolt. **27**(1), 3–12 (2019)
10. R. Hemmatzadeh, A. Mohammadi, Improving optical absorptivity of natural dyes for fabrication of efficient dye-sensitized solar cells. J. Theor. Appl. Phys. **7**(1), 57 (2013)
11. S. Çakar, M. Özacar, Fe–tannic acid complex dye as photo sensitizer for different morphological ZnO based DSSCs. Spectrochim Acta A Mol Biomol Spectrosc. **163**, 79–88 (2016)
12. D.S. Tribawono, D. Wibowo, M. Nurdin, Electrochemical profile degradation of amino acid by flow system using TiO_2/Ti nanotubes electrode. Anal. Bioanal. Electrochem. **8**(6), 761–776 (2016)
13. J. Li, W. Wu, J. Yang, J. Tang, Y. Long, J. Hua, Effect of chenodeoxycholic acid (CDCA) additive on phenothiazine dyes sensitized photovoltaic performance. Sci. China Chem. **54**(4), 699–706 (2011)
14. Z.S. Wang, Y. Cui, Y. Dan-oh, C. Kasada, A. Shinpo, K. Hara, Thiophene-functionalized coumarin dye for efficient dye-sensitized solar cells: electron lifetime improved by coadsorption of deoxycholic acid. J. Phys. Chem. C **111**(19), 7224–7230 (2007)
15. S. Qu, W. Wu, J. Hua, C. Kong, Y. Long, H. Tian, New diketopyrrolopyrrole (DPP) dyes for efficient dye-sensitized solar cells. J. Phys. Chem. C **114**(2), 1343–1349 (2010)
16. J.H. Yum, S.R. Jang, R. Humphry-Baker, M. Grätzel, J.J. Cid, T. Torres, M.K. Nazeeruddin, Effect of coadsorbent on the photovoltaic performance of zinc pthalocyanine-sensitized solar cells. Langmuir **24**(10), 5636–5640 (2008)
17. R. Ahmad, M.H. Sayyad, N. Nasr, S. Sajjad, Efficiency enhancement of dye sensitized solar cells with a low cost co-adsorbent in N719 Dye. Int. J. Sustain. Energy **5**, 46–50 (2016)
18. J. Siriporn, K. Sirithip, N. Prachumrak, R. Tarsang, T. Sudyoadsuk, S. Namuangruk, N. Kungwan, V. Promarak, T. Keawin, Significant enhancement in the performance of porphyrin for dye-sensitized solar cells: aggregation control using chenodeoxycholic acid. N. J. Chem. **41**(15), 7081–7091 (2017)
19. C.D. Heatubun, J. Dransfield, T. Flynn, S.S. Tjitrosoedirdjo, J.P. Mogea, W.J. Baker, A monograph of the betel nut palms (Areca: Arecaceae) of East Malesia. Bot. J. Linn. Soc. **168**(2), 147–173 (2012)
20. J. Shrestha, T. Shanbhag, S. Shenoy, A. Amuthan, K. Prabhu, S. Sharma, Antiovulatory and abortifacient effects of *Areca catechu* (betel nut) in female rats. Indian J. Pharmacol. **42**(5), 306–311 (2010)
21. H.K. Amarasinghe, U.S. Usgodaarachchi, N.W. Johnson, R. Lalloo, Betel-quid chewing with or without tobacco is a major risk factor for oral potentially malignant disorders in Sri Lanka: a case-control study. Oral Oncol. **46**(4), 297–301 (2010)
22. J.S. Jung, Making of natural dyeing scarves by tie-dyeing technique. In *MATEC Web of Conferences*, vol. 108, (EDP Sciences, 2017), p. 03006
23. A.S. Najm, A.B. Mohamad, N.A. Ludin, The extraction and absorption study of natural dye from *Areca catechu* for dye sensitized solar cell application. Am. Inst. Phys. **020019**, 020019 (2017)
24. X. Wang, M. Xi, F. Zheng, B. Ding, H. Fong, Z. Zhu, Reduction of crack formation in TiO_2 mesoporous films prepared from binder-free nanoparticle pastes via incorporation of electrospun SiO_2 or TiO_2 nanofibers for dye-sensitized solar cells. Nano Energy **12**, 794–800 (2015)
25. E. Yamazaki, M. Murayama, N. Nishikawa, N. Hashimoto, M. Shoyama, O. Kurita, Utilization of natural carotenoids as photosensitizers for dye-sensitized solar cells. Sol. Energy **81**(4), 512–516 (2007)
26. M.F. Abdullah, R. Zulkifli, Z. Harun, S. Abdullah, W. Ghopa, W. Aizon, A. Soheil Najm, N. Humam Sulaiman, Impact of the TiO_2 nanosolution concentration on heat transfer enhancement of the twin impingement jet of a heated aluminum plate. Micromachines **10**(3), 176 (2019)
27. D. Barraza-Jiménez, A.M. Cruz, L. Saucedo-Mendiola, S.I. Torres-Herrera, A.P. Mendiola, E.M. Quiñones, R.A. Corral, M.E. Frías-Zepeda et al., in *Solvent Effects on Dye Sensitizers Derived from Anthocyanidins for Applications in Photocatalysis*, Solvents and Solvent Effects (IntechOpen, 2019)
28. R. Abarca-Vargas, C.F.P. Malacara, V.L. Petricevich, Characterization of chemical compounds with antioxidant and cytotoxic activities in bougainvillea x buttiana holttum and standl, (var. Rose) extracts. Antioxidants **5**(4), 45 (2016)
29. C. Lee, W. Lee, C. Yang, High efficiency of dye-sensitized solar cells based on ruthenium and metal-free dyes. Int. J. Photoenergy (2013). https://doi.org/10.1155/2013/250397
30. H.C. Hassan, Z.H.Z. Abidin, F.I. Chowdhury, A.K. Arof, A high efficiency chlorophyll sensitized solar cell with quasi solid PVA based electrolyte. Int. J. Photoenergy (2016). https://doi.org/10.1155/2016/3685210
31. N. Ravin, *Engineered Carbohydrate-Based Materials for Biomedical Applications: Polymers, Surfaces, Dendrimers, Nanoparticles, and Hydrogels* (Wiley, Hoboken, 2011)
32. K. Hosseinpanahi, M. Hossein, J. Feizy, M.R. Golzarian, Dye-sensitized solar cell using saffron petal extract as a novel natural sensitizer. J. Sol. Energy Eng. **139**, 3–7 (2017)
33. T. Oguchi, N. Sasaki, T. Hara, Y. Tozuka, K. Yamamoto, Differentiated thermal crystallization from amorphous chenodeoxycholic acid between the ground specimens derived from the polymorphs. Int. J. Pharm. **253**(1–2), 81–88 (2003)
34. M. Ismail, N.A. Ludin, N.H. Hamid, The effect of chenodeoxycholic acid (CDCA) in Mangosteen (*Garcinia mangostana*) pericarps sensitizer for dye-sensitized solar cell (DSSC). J. Phys. **1083**(1), 012018 (2018)
35. C.C. Mercado, F.J. Knorr, J.L. McHale, S.M. Usmani, A.S. Ichimura, L.V. Saraf, Location of hole and electron traps on nanocrystalline anatase TiO_2. J. Phys. Chem. C **116**(19), 10796–10804 (2012)
36. Y. Huang, J. Du, J. Zhang, Z. Liu, B. Han, T. Jiang, Controlled synthesis of $AgTiO_2$ core−shell nanowires with smooth and bristled surfaces via a one-step solution route. pdf (2006)
37. S. Kavitha, K. Praveena, M. Lakshmi, A new method to evaluate the feasibility of a dye in DSSC application. Int. J. Energy Res. **41**(14), 2173–2183 (2017)
38. Y. Li, S.H. Ku, S.M. Chen, M.A. Ali, F.M.A. AlHemaid, Photoelectrochemistry for red cabbage extract as natural dye to develop a dye-sensitized solar cells. Int. J. Electrochem. Sci. **8**(1), 1237–1245 (2013)
39. G. Zhang, H. Bala, Y. Cheng, D. Shi, X. Lv, Q. Yu, P. Wang, High efficiency and stable dye-sensitized solar cells with an organic chromophore featuring a binary π-conjugated spacer. Chem. Commun. **16**, 2198–2200 (2009)
40. Q.P. Wu, Y.J. Xu, X.B. Cheng, M. Liang, Z. Sun, S. Xue, Synthesis of triarylamines with secondary electron-donating groups for dye-sensitized solar cells. Sol. Energy **86**(2), 764–770 (2012)
41. M.S. Su'ait, M.Y.A. Rahman, A. Ahmad, Review on polymer electrolyte in dye-sensitized solar cells (DSSCs). Sol. Energy **115**, 452–470 (2015)

42. S. Guo, D. Wen, Y. Zhai, S. Dong, E. Wang, Platinum nanoparticle ensemble-on- rapid synthesis, and used as new sensing. ACS Nano **4**(7), 3959–3968 (2010)
43. R. Vittal, K. Ho, Zinc oxide based dye-sensitized solar cells: a review. Renew. Sustain. Energy Rev. **70**, 920–935 (2017)
44. H.F. Zarick, O. Hurd, J.A. Webb, C. Hungerford, W.R. Erwin, R. Bardhan, Enhanced efficiency in dye-sensitized solar cells with shape-controlled plasmonic nanostructures SI. ACS Photon. **1**, 806–811 (2014)
45. R. Kushwaha, P. Srivastava, L. Bahadur, Natural pigments from plants used as sensitizers for TiO_2 based dye-sensitized solar cells. J. Energy (2013). https://doi.org/10.1155/2013/654953
46. A. Carissa, M.S. Esteban, E.P. Enriquez, Graphene—anthocyanin mixture as photosensitizer for dye-sensitized solar cell. Sol. Energy **98**, 392–399 (2013)
47. P.R. Barnes, A.Y. Anderson, M. Juozapavicius, L. Liu, X. Li, E. Palomares, Factors controlling charge recombination under dark and light conditions in dye sensitised solar cells. Phys. Chem. Chem. Phys. **13**(8), 3547–3558 (2011)
48. D. Pugliese, N. Shahzad, A. Sacco, G. Musso, A. Lamberti, G. Caputo, E. Tresso, S. Bianco, C.F. Pirri, Fast TiO_2Sensitization using the semisquaric acid as anchoring group. Int. J. Photoenergy (2013). https://doi.org/10.1155/2013/871526
49. J.A. Mikroyannidis, P. Suresh, M.S. Roy, G.D. Sharma, New photosensitizer with phenylenebisthiophene central unit and cyanovinylene 4-nitrophenyl terminal units for dye-sensitized solar cells. Electrochim. Acta **56**(16), 5616–5623 (2011)
50. G. Calogero, G. Di Marco, Red sicilian orange and purple eggplant fruits as natural sensitizers for dye-sensitized solar cells. Sol. Energy Mater. Sol. Cells **92**, 1341–1346 (2008)
51. H. Zhou, L. Wu, Y. Gao, T. Ma, Dye-sensitized solar cells using 20 natural dyes as sensitizers. J. Photochem. Photobiol. A **219**(2–3), 188–194 (2011)
52. N.M. Gómez-Ortíz, I.A. Vázquez-Maldonado, A.R. Pérez-Espadas, G.J. Mena-Rejón, J.A. Azamar-Barrios, Dye-sensitized solar cells with natural dyes extracted from achiote seeds. Sol. Energy Mater. Sol. Cells **94**, 40–44 (2010)
53. K. Wongcharee, V. Meeyoo, S. Chavadej, Dye-sensitized solar cell using natural dyes extracted from rosella and blue pea flowers. Sol. Energy Mater. Sol. Cells **91**(7), 566–571 (2007)
54. R.A.M. Ali, N. Nayan, Fabrication and analysis of dye-sensitized solar cell using natural dye extracted from dragon fruit. INT J INTEGR ENG **2**(3), (2010)
55. W. Hao, Y. Hsun, L. Gaik, M. Hsiung, Commercial and natural dyes as photosensitizers for a water-based dye-sensitized solar cell loaded with gold nanoparticles. J. Photochem. Photobiol. A **195**, 307–313 (2008)
56. T.S. Senthil, N. Muthukumarasamy, D. Velauthapillai, S. Agilan, M. Thambidurai, R. Balasundaraprabhu, Natural dye (cyanidin 3-O-glucoside) sensitized nanocrystalline TiO_2 solar cell fabricated using liquid electrolyte/quasi-solid-state polymer electrolyte. Renew. Energy **36**, 2484–2488 (2011)
57. H. Chang, H.M. Wu, T.L. Chen, K.D. Huang, C.S. Jwo, Y.J. Lo, Dye-sensitized solar cell using natural dyes extracted from spinach and ipomoea. J. Alloys Compd. **495**(2), 606–610 (2010)
58. K. Eb, JaSiM, Natural dye-sensitized solar cell based on nanocrystalline TiO_2. Sains Malays. **41**(8), 1011–1016 (2012)
59. K.V. Hemalatha, S.N. Karthick, C.J. Raj, N. Hong, S. Kim, H. Kim, Performance of *Kerria japonica* and *Rosa chinensis* flower dyes as sensitizers for dye-sensitized solar cells. Spectrochim. Acta A **96**, 305–309 (2012)